Innovative Composite Precast Prestressed Precambered U-Shaped Concrete Deck for Belgium's High Speed Railway Trains

Stéphanie Staquet, Ph.D.
Postdoctoral Researcher
Department of Civil Engineering
Université Libre de Bruxelles
Brussels, Belgium

Guy Rigot
Administrator-Director
Ets Ronveaux s.a.
Ciney, Belgium

Henri Detandt
Manager
Bridge Department
Tucrail s.a.
Brussels, Belgium

Bernard Espion, Ph.D.
Professor
Department of Civil Engineering
Université Libre de Bruxelles
Brussels, Belgium

Construction of single-track high speed rail lines in Brussels, Belgium, required an innovative precast, prestressed precambered composite trough bridge deck system to meet stringent site specifications. The resultant U-shaped bridge deck – a design born of the earlier Preflex and Flexstress beams, briefly described herein – permits spans as long as 92 ft (28 m). Variability in camber between measured data and that of traditionally computed methods led to a study to better evaluate time-dependent effects in concrete composite structures. This article presents a method of analysis to measure the creep and shrinkage effects on the long-term behavior of the decks. Strain measurements of the bridge deck 2½ years after construction are also compared with the theoretical values. The step-by-step method showed a better agreement with the measured strains than the values calculated by the age-adjusted effective modulus method. It is concluded that the research program on time-dependent effects has been successful and that the experimental results have in general agreed with the theoretical values.

During the past decade, an innovative composite precast, prestressed U-shaped bridge deck has been developed for use in the construction of the high speed railway system in Belgium (see Fig. 1) and for replacing the old structural steel bridges that are being phased out. The railway system, centered in Brussels, connects London, Paris, Amsterdam and Cologne (Köln) – one of the most densely

Fig. 1. An innovative composite precast, prestressed precambered U-shaped concrete deck is providing the structural support for the high speed railway trains in Belgium. (Courtesy of Tucrail)

populated transportation corridors in the world. The maximum speed attained by these rapid modern trains in open areas is 186 miles per hour (300 km/h).

The new composite design is basically a precast, precambered, prestressed concrete-steel bridge deck with a U-shaped, or trough, cross section that is built in two phases. The origin of this design goes back to the Preflex and Flexstress beams, systems also developed in Belgium about 50 years ago. The new section represents the last significant development in the evolution of composite precambered beams. However, it should be emphasized that the new deck system is substantially different from the earlier Preflex and Flexstress beams.

In order to obtain a clear understanding of the new deck system presented here, it is necessary to review the origins and basic principles of this hybrid beam. Therefore, a brief history of the development of the Preflex and Flexstress beams is first presented.

HISTORICAL BACKGROUND

Preflex Beam

The first composite precambered beam, called the Preflex beam, was invented by the Belgian engineer, A. Lipski, with assistance from L. Baes.[1] The first such project using this beam dates back to 1951. The two best known structures are the Southern Tower (Tour du Midi) and the Berlaymont Building, both in Brussels. The first building used 144 Preflex beams[2] with spans of 131 ft (40 m) and the second building used 319 Preflex beams.[3]

The typical construction sequence of a Preflex beam with a 109 ft (33.4 m) span is as follows (see Fig. 2):

a. In the plant, setup a steel I-girder with a precamber of 11½ in. (294 mm) supported at each end bearing.
b. Preflex (prebend) the steel girder by applying two concentrated loads of 417 kips (1854 kN) at one-quarter and three-quarters of the span.

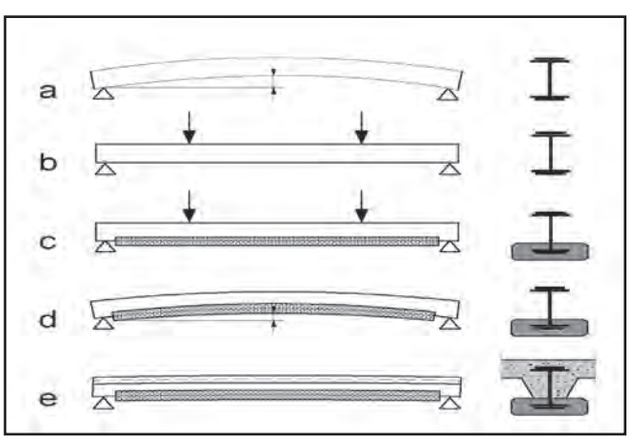

Fig. 2. Schematic showing construction stages of Preflex (precambered) beam.

c. Cast the first phase of high strength concrete (HSC) at the level of the bottom flange of the steel girder while keeping in place the loads of the preflexed phase of the girder.
d. Seven days after casting the concrete, remove the preflexed loads. As a result, the beam goes up, the precamber becomes smaller than the original precamber, and the concrete is now subjected to compression.
e. Cast the second phase concrete on site.

The first and second concrete phases significantly increase the stiffness of the composite beam as compared to the stiffness of the steel girder alone. Since the concrete of the bottom flange is subjected to compression before the application of service loads, this concrete is useful in this part of the beam because it satisfies the requirement of no cracking in the concrete.

This system has been particularly successful in Belgium because it can accommodate long spans, has a minimal construction depth, and offers excellent fire resistance. During the past 50 years, the Preflex beam has performed excellently.

Flexstress Beam

The next significant improvement in the evolution of composite precambered beams was the introduction of additional prestressing to the beam which expanded the range of applications of the prestressed composite system. The new method, known as Flexstress, was pioneered by the Ronveaux Company. Precast, prestressed Flexstress beams were used in the construction of the bridge over the Lixhe Dam across the Maas River in 1986. These beams have a span of 154 ft (47 m).[4] A typical Flexstress beam in a precasting yard is shown in Fig. 3.

The Flexstress system incorporates all of the advantages that come from combining the two principal elements of structural concrete, namely, concrete and steel. The concrete can be prestressed using pretensioning and the steel beam can be prestressed or precambered. It is, therefore, the combination of all these techniques that produces the maximum structural efficiency.

Fig. 3. Flexstress (precambered) beam at precasting yard. (Courtesy of Ronveaux Company)

A typical cross section of a Flexstress beam is shown in Fig. 4.

The basis of the Flexstress beam is a high strength steel A572 Grade (S355) precambered girder from which the residual stresses can be removed by a preliminary series of loading/unloading cycles. During this phase, the tensile stress reaches 85 percent of the yield strength.

Next, external tendons acting at the level of the bottom flange of the steel girder are attached. The purpose of this loading phase (called "turbo-preflexion") is to increase the prebending capacity of the girder.

This prebending comprises the application of two loads on the girder at one-quarter and three-quarters of the span. At the end of this operation, the

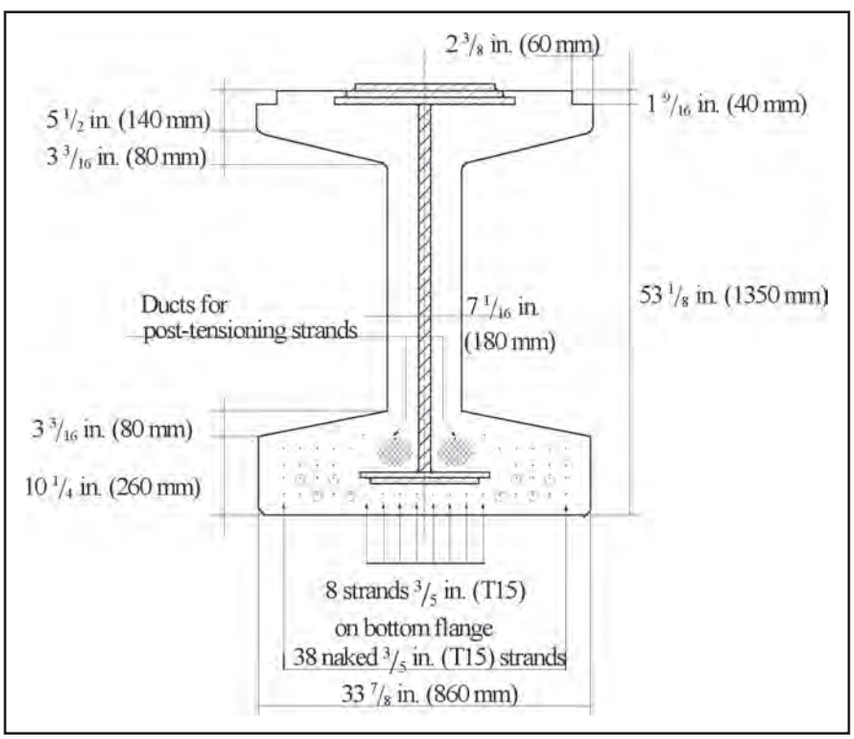

Fig. 4. Cross section of Flexstress (pretensioned, post-tensioned) beam.

girder is completely encased in concrete. When the minimum required concrete strength is reached, the two loads are removed and prestressing (using pretensioning) is applied on the bottom flange.

To increase the prestressing force that can be applied to the beam, a temporary anti-prestressing (decompression) device is placed at the top of the girder. This precaution is necessary in the event the beam supports are placed too closely during transportation, thus causing large cantilever moments. The temporary prestressing is removed prior to placing the top slab. Finally, after the top slab has hardened sufficiently, the composite beam is post-tensioned.

It needs to be emphasized that Flexstress is not simply the presence of two known techniques. Rather, it is the innovative combination of two basic principles of prestressing and prebending, namely, the application of prestressing on the bottom flange of the steel beam (turbo-preflexion) and the temporary decompression (anti-prestressing) on the concrete, together with the full encasing of the beam during prefabrication.

U-SHAPED BRIDGE DECK FOR BRUSSELS SOUTH STATION

The U-shaped bridge deck section was conceived and designed in the early 1990s with the intent of the bridge deck being used for the high speed rail superstructure of the Brussels South Station. The entrance of the high speed rail line in the station involved the construction of a specific terminal and a direct link between the rail line and the new terminal. More than 2 miles (3 km) of viaducts with single track had to be built in a busy urban area. Therefore, a completely new type of bridge deck had to be developed quickly to meet this transportation challenge.

The Brussels South Station is the most important railway station in Belgium. For this reason, the Brussels terminal was chosen as the center for Eurostar Trains coming in from London and also to be the main intermediate station for the Thalys Trains between Paris and Amsterdam, or between Paris and Cologne (Köln). Before this project was started, there were 22 tracks with platforms in the Brussels South Station. Four of them did not have a link with the Brussels North Station.

After the station is upgraded, six tracks with platforms will be used by the high speed trains, and four of these tracks will have a direct link with the Brussels North Station. Note that the western side of the station was chosen as the location of the high speed train platforms.

Since the trains coming in from France arrive at the eastern side of the station, it became necessary to establish a direct link between the new high speed line and a new specific terminal for high speed trains. To avoid crossing the railway tracks at the same level and also to improve the existing domestic network, several viaducts had to be built. Consequently, many requirements had to be taken into consideration:

- A minimal construction depth [distance between the lower level of the ballast (gravel fill) and the lower level of the bridge deck] is necessary to reduce the slope of the crossing tracks and to have enough clearance under the tracks for the entrance hall of the new station.
- Railway traffic on the existing tracks that must be crossed by the new viaducts could not be interrupted for extended periods.
- The disturbance during construction had to be reduced to a minimum.
- The noise level caused by the passing trains on the new viaducts also had to be reduced in the urban environment.

To meet the above requirements, an innovative system, comprising precast composite trough (U-shaped) bridge decks, has been developed and applied successfully on single rail track. Indeed, the Belgian National Railways introduced this precast system in 1988 to replace the old steel bridges. Since then, excellent service has been experienced. The concrete deck sections are prefabricated in a plant to ensure high quality control and also to reduce on-site erection time.[5]

EXTENSION AND UPGRADING OF BRUSSELS SOUTH STATION

The Brussels South Station was built between 1945 and 1950. On its western side, the tracks and platforms were supported by steel viaducts that were about 20 ft (6 m) higher than the main hall for passengers at street level.

Because the space under the tracks was reserved for passengers, this part of the station was chosen as a specific terminal for the high speed trains. In particular, Trains 1 and 2, which were used by the Eurostar Trains to London

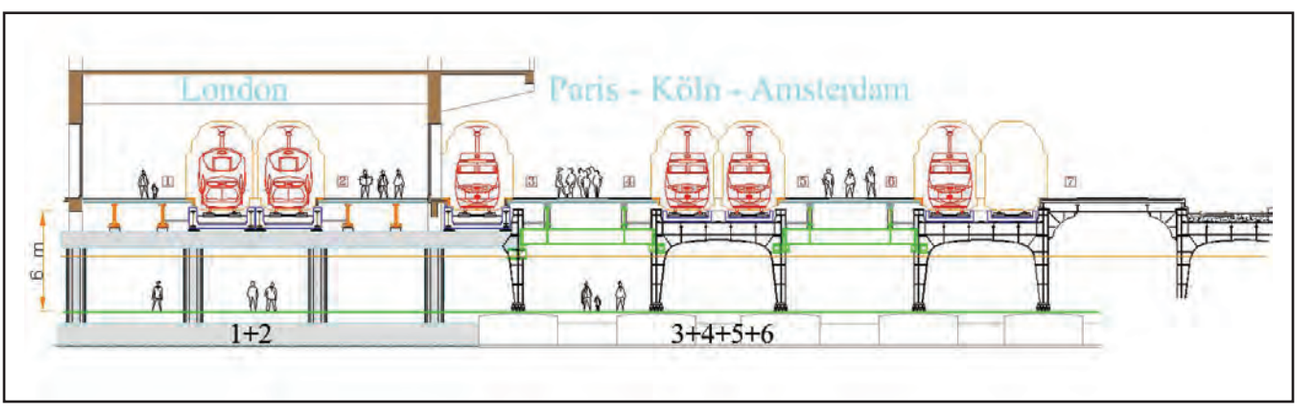

Fig. 5. Cross section of Brussels South Station showing location of tracks and platforms. (Courtesy of Tucrail)

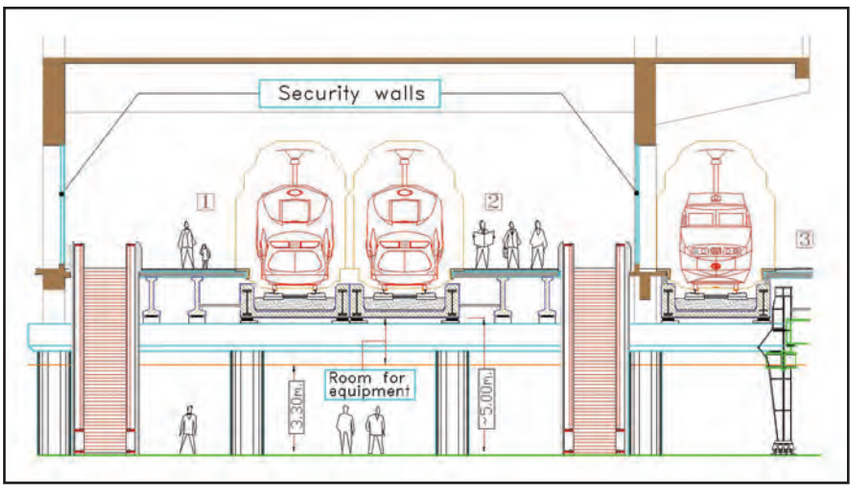

Fig. 6. Cross section of station for Eurostar trains to London showing precast, prestressed U-shaped deck supporting railway tracks and platforms. (Courtesy of Tucrail)

Fig. 7. Erection of precast, prestressed U-shaped deck at Brussels South Station using launching truss. (Courtesy of Tucrail)

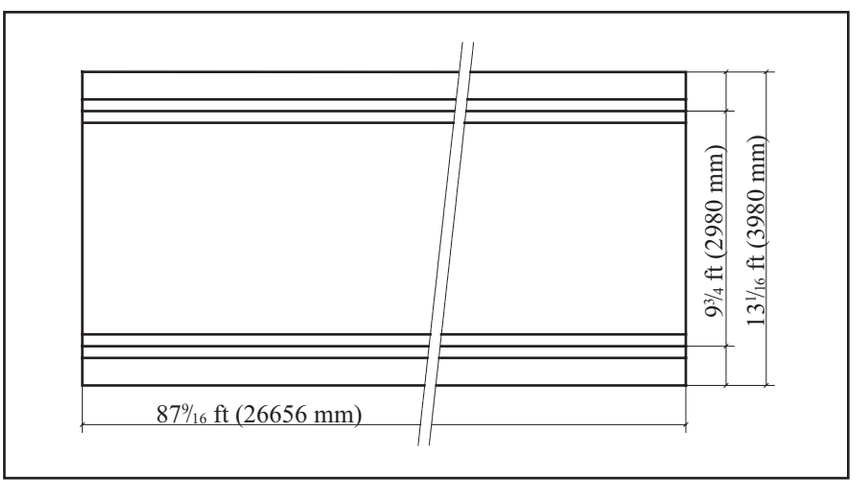

Fig. 8. Plan view of simplified length of U-shaped deck with span of 87 9/16 ft (26.65 m).

(see Fig. 5), had to be isolated for security reasons. Therefore, Station Tracks 1, 2, and 3 had to be removed. In addition, the platforms had to be extended northwards.

Maximizing space – To obtain the maximum possible space for passengers and equipment (see Fig. 6), a novel combination of trough bridge decks for railway track and two precast, prestressed concrete beams connected with a reinforced concrete transfer slab were used. Also, to decrease noise levels and to produce a smooth train ride, high quality elastomeric rubber bearings were installed under the concrete sleepers (railroad ties).

The project included the construction of about 58 bridge decks with spans varying from 59 to 75 ft (18 to 23 m). These deck sections were prefabricated in a plant and then transported by train to the station.

Deck launching – To erect the deck sections, a launching truss, 167 ft (51 m) long, was used. The launcher was equipped with a roller track and was supported by three gantries (see Fig. 7). Two trolleys, with lifting jacks, could move the deck sections from the train bogies to their final installation. The fabrication process and launching method significantly reduced construction time and, in general, made the entire operation very efficient.

Because the train tracks at the entrance to the Brussels South Station are so heavily used, interruption of rail traffic was only allowed during a very few hours of the night. Another advantage of prefabrication is that city road traffic in the vicinity of the station was barely disturbed.

Eight viaducts – So far, eight single track viaducts have been constructed near the entrance of the high speed line to the Brussels South Station. Most of the piers are circular cast-in-place (CIP) concrete columns supporting a specially designed precast concrete cross-head. The superstructure consists of precast trough bridge decks for single track rail lines. They have a depth of 51 in. (1.3 m) and a maximum span of 85 ft (26 m) (see Figs. 8 and 9).

The deck sections are prefabricated in a plant and are transported by train on bogies to the project site. With the aid of cranes, the sections are then

placed on elastomeric bearing pads (see Figs. 10 and 11). A typical cross section of the viaduct is shown in Fig. 12. An overview of a single-track viaduct is shown in Fig. 13.

The structures supporting the train tracks and pedestrian footpaths are clearly separated. In the case of double tracks, both the substructure and superstructure are separated from each track. Also, each bridge deck has only one footpath. In the case of a single track, a footpath is built as a safety precaution on each side of the bridge deck. When viaducts carry tracks with a small curvature radius, independent viaducts for single track can accommodate them easily.

All these viaducts support ballasted (gravel filled) tracks with UIC 60 rails laid on concrete sleepers (railroad ties). Since the bridge decks are simply supported on piers and because the track is laterally stable, continuous welded rails are used without rail expansion joints in the track. This feature is important from the viewpoint of passenger comfort, safety, noise abatement and maintenance.

Measurements of vertical acceleration in the high speed trains traveling at 56 miles per hour (90 km/h) have already been made on the first completed viaduct. The results show that the vertical acceleration is well within the allowable values corresponding to "very good level of comfort," given by the Eurocodes.

The construction of the eight viaducts has taken about ten years to complete because the consecutive phases of the project cannot be carried out simultaneously. Altogether, a total of 150 bridge decks will be needed to accommodate the various links.[5] The entire project is scheduled for completion by the end of 2005.

CONSTRUCTION PHASES OF COMPOSITE U-SHAPED BRIDGE DECKS

Preflexion or Girder Prebending (see Fig. 14)

The composite steel-concrete trough, or U-shaped bridge deck, has a width limited to 13⅛ ft (4 m) due to transportation restrictions. Two hot-rolled or welded steel girders are curved (or

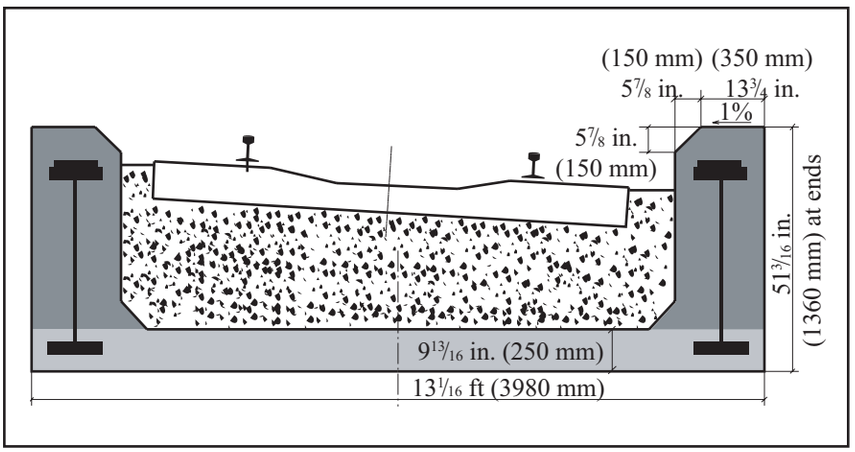

Fig. 9. Cross section of U-shaped deck at midspan with width of 13¹⁄₁₆ ft (3980 mm). (Courtesy of Tucrail)

Fig. 10. Two cranes are used to install U-shaped deck near Brussels South Station. (Photograph by Bernard Espion)

Fig. 11. Installation of U-shaped deck near Brussels South Station. (Courtesy of Tucrail)

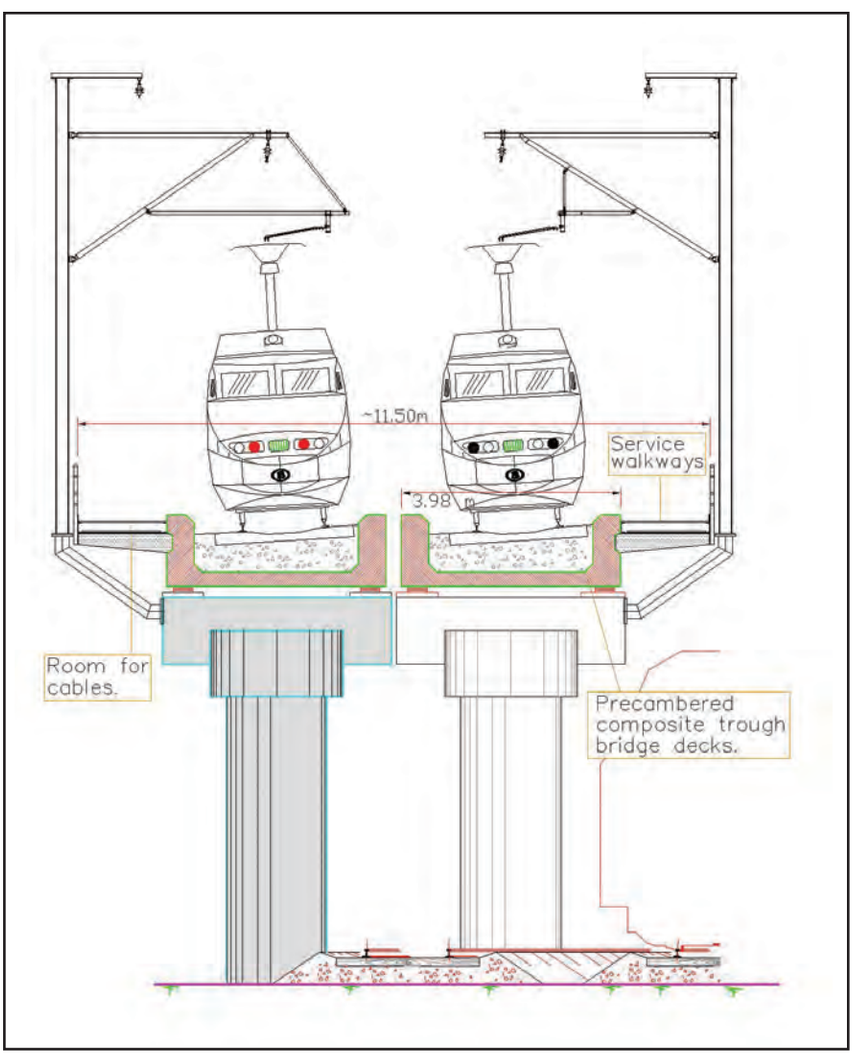

Fig. 12. Cross section of viaduct. (Courtesy of Tucrail)

bent) longitudinally in the plant to produce an initial camber (see Fig.15a). The girders are then placed in a special assembly at the workshop. The upper flanges of the girders are fixed to prevent lateral buckling.

Elastification phase – The first step in the production process is the so-called "elastification phase" of the steel girders that removes residual stresses by successive loading/unloading cycles (see Fig. 15b). To remove the residual stresses, two mechanically induced loads are applied on each girder at one-quarter and three-quarters of the span in order to completely flatten the girders and thus to reduce the camber to zero (see Fig. 15c).

Note that in all cases, the stress level in the girders during this preflexion (prebending) phase is less than 80 percent of the yield strength. These steel girders will become integrated as the two sides of the U-shaped bridge deck.

Casting of Bottom Slab

A few hours after prebending the steel girders, the casting of the bottom slab of the deck takes place. First, mild steel reinforcing bars with a characteristic yield strength of 72.5 ksi (500 MPa) and bare (uncoated) prestressing tendons are placed in a longitudinal direction along the bottom

Fig. 13. Side view of single-track viaduct, extending about 495 ft (151 m) in length. (Courtesy of Tucrail)

of the section (see Fig. 14). Next, the tendons are tensioned in the space that will be filled by the 9.8 in. (250 mm) deep bottom slab concrete.

Fig. 15c shows that the bottom flanges of the girders are encased in the concrete; for this reason, neither the prestressing tendons nor the mild reinforcing steel require any protection. The fresh concrete is heat cured at a temperature of 113°F (45°C).

Prestressing of Bottom Slab and Second Concrete Placement

When the bottom slab concrete reaches a strength of 6527 psi (45 MPa) for 6 x 6 in. (150 x 150 mm) cubes, it is prestressed by releasing the prebending of the girders and transferring the prestressing force from the tendons to the composite structure (see Fig. 15d). On the following day, the remaining exposed parts of the steel girders are enclosed in a second concrete placement to complete the webs (see Fig. 15e).

ADVANTAGES OF PRECAMBERED PRESTRESSED U-SHAPED DECKS

Two specific requirements had to be fulfilled in the design of the U-shaped bridge decks: minimize the construction depth of the deck and maximize the bridge span length. In the following, traditionally designed structures without steel girders or prestressing are compared with the U-shaped bridge deck to demonstrate its advantages.

Fig. 14. Precambered (preflexion) stage of steel beams showing prestressing tendons and reinforcing steel in plant. (Photograph by Bernard Espion)

Benefits of Steel Girders on Slab Depth

In the design of U-shaped bridge decks, the precambered steel girders play an important role because they have a significant effect on the carrying capacity of the structure. Three types of bridge decks using a 7250 psi (52 MPa) concrete have been chosen to illustrate the beneficial influence of incorporating steel girders.

Types A, B and C Bridge Decks – Type A is a trough-shaped bridge deck without steel girders with the following dimensions: 4⅛ ft (1.26 m) high, 13⅛ ft (4.0 m) wide, and a 9$^{3}/_{16}$ in. (233 mm) deep slab. Type B is a trough-shaped bridge deck with the same di-

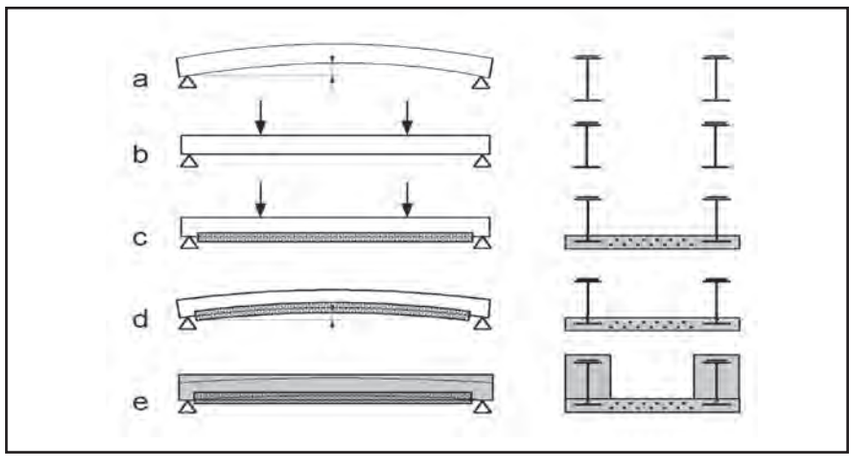

Fig. 15. Schematic showing construction stages of U-shaped deck.

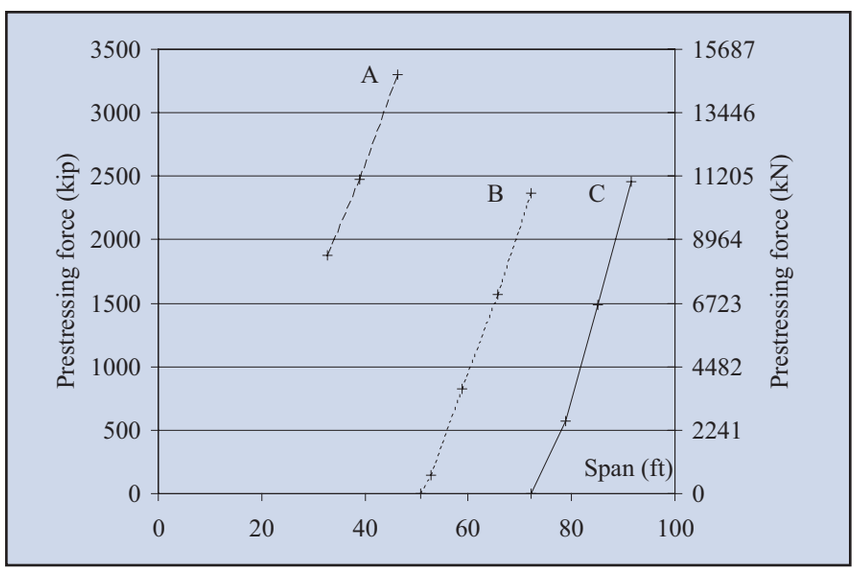

Fig. 16. Variation of required prestressing force for three types of bridge decks as a function of their spans.

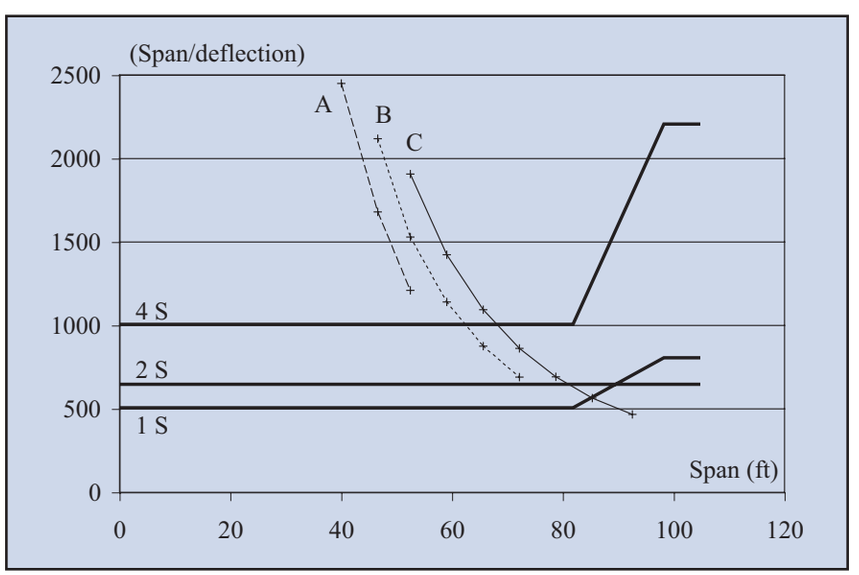

Fig. 17. Variation of span-to-deflection ratio for three types of bridge decks as a function of their spans.

mensions as Type A, but with two precambered high strength steel girders A572 Grade (S355), each weighing 240 lb per ft (357 kg/m). Type C is the same as Type B, but with stronger girders, each weighing 480 lb per ft (714 kg/m).

In Figs. 16 and 17, the required prestressing force for each of the three types of bridge decks is computed in order to ensure that ultimate limit state requirements according to the Eurocodes are met, and also to check that no concrete decompression occurs under UIC Load Model 71. In Figs. 16, 17, 18 and 19, these bridge decks are subjected to self-weight, ballast, and a UIC load.

Maximum span length – By using the Type A bridge deck, a maximum span of 46 ft (14 m) can be reached, whereas a maximum span of 92 ft (28 m) is possible with the Type C deck with precambered and prestressed steel girders. Fig. 17 shows that for a given span-to-deflection ratio, a longer span can be achieved with Type C or B decks than with Type A, as the stiffness of the bridge deck is greatly increased by the addition of steel girders.

In Figs. 17 and 19, the bold lines 1S, 2S and 4S represent the lowest acceptable span-to-deflection ratios according to the deflection requirements of UIC (Leaflet 776-3) for train speeds between 75 and 124 miles per hour (120 and 200 km/h). Symbols 1S, 2S and 4S represent a structure with one, two and four spans, respectively.

Slab depth – Fig. 18 shows the influence of deck type on slab depth. Types D and E are similar in design to Type C, but use 8700 psi (60 MPa) concrete instead. The slab depths for Types E and D are 9$\frac{3}{16}$ and 11$\frac{3}{16}$ in. (233 and 300 mm), respectively. Fig. 18 shows that the increase of slab depth has no significant effect on the maximum span length. Consequently, the Type E slab depth was selected.

Fig. 19 shows that an increase in slab depth has a negligible influence on the stiffness of the bridge deck. Even when taking the deflection requirement into account, very long spans with shallow construction depths can be achieved by using this type of structure.

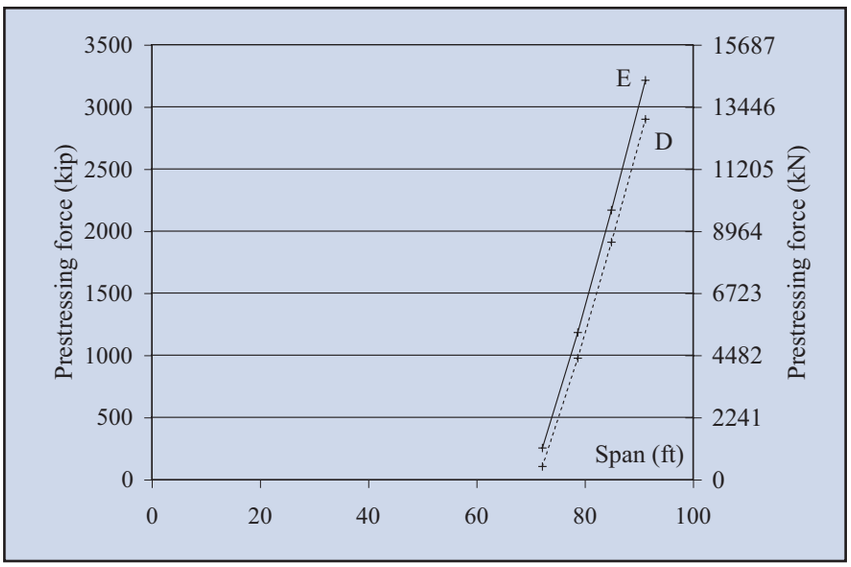

Fig. 18. Variation of required prestressing forces for two U-shaped bridge decks with different slab depths as a function of their spans.

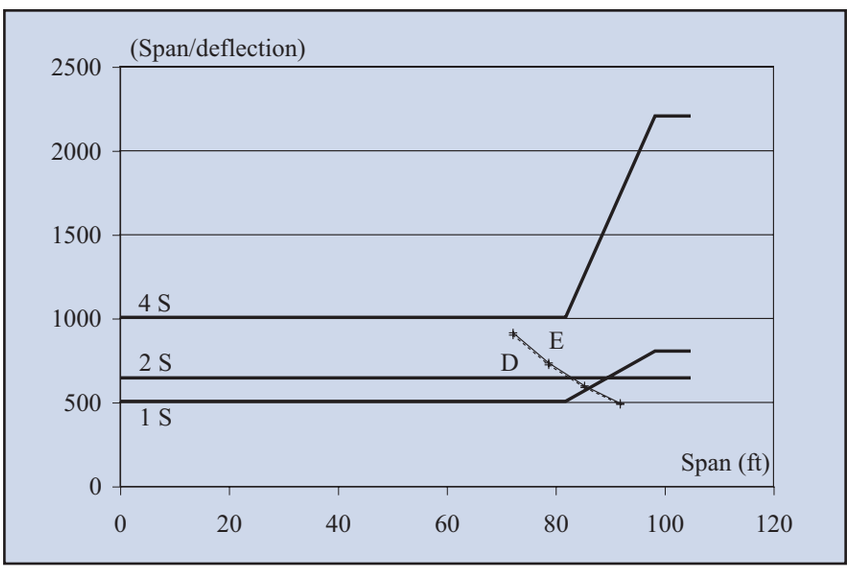

Fig. 19. Variation of span-to-deflection ratio for two U-shaped bridge decks with different slab depths as a function of their spans.

Typical Decks Versus U-Shaped Decks With Steel Girders

In order to quantify other advantages of U-shaped decks with steel girders, some characteristics of a typical prestressed precambered trough bridge, Deck F, are listed in Fig. 20 and compared with a similar composite deck with simply-encased steel girders (Deck G). Bridge Deck F corresponds to the Type B above.

Bridge Deck G includes eight parallel HEB 900 steel girders of A572 Grade (S355) that are fully encased in 7250 psi (50 MPa) concrete. The total width of both decks is 13⅛ ft (4.0 m). Each bridge deck has a 65⅝ ft (20.0 m) span length and is subjected to self-weight, ballast, and UIC loading. The computations have taken into account the ultimate limit states, and in the case of prestressed concrete Deck F, have also considered that concrete remains fully compressed according to the UIC Load Model 71.

Fig. 20 illustrates that for the same span length, width, loading, self-weight, and member depth, the prestressed precambered trough bridge Deck F requires considerably less reinforcing steel and concrete than that required for Bridge Deck G, which consists of simply encased steel girders.

Table 1 provides a summary of the major properties of the U-shaped bridge deck.

DESIGN OF NEW U-SHAPED BRIDGE DECKS

Previously, the trough bridge deck was designed at the service limit state using a simple, classical computation method. This earlier method takes into account the time-dependent effects of concrete within the framework of a pseudo-elastic analysis with a variable steel-to-concrete modular ratio, m. This method is similar to the well-known effective modulus method (EMM), in which the concrete modulus of elasticity is replaced by a variable-reduced modulus as a function of time.

In the past ten years, this EMM type method was used to construct at least 400 bridge decks in Belgium. Half of these bridges were used to build the Brussels South Station infrastructure, and the other half were erected on the Belgian Railway Network as replacements for old steel truss bridges with double tracks.

While these bridge decks have performed according to expectations, some variability has been observed between the measured and computed camber just after the transfer of prestressing. At prestress transfer, time-dependent effects do not yet have a significant impact, and the pseudo-elastic computation should provide realistic modeling. To explain the observed variability in camber, a multivariable statistical analysis was conducted on 42 bridge decks, and is a major focus of this paper.

Significant Variables

Before beginning the statistical analysis, the variables assumed to be linked to bridge deck camber were determined. The first step in understanding structural behavior is to analyze the material characteristics of the concrete mixture used. The concrete compressive strength, f'_c, was measured on 6 x 6 in. (150 x 150 mm) cubes.

The concrete mixture for both concrete phases was identical:

- Sand (from the Maas River): 1206 lb per cu yd (715 kg/m^3)

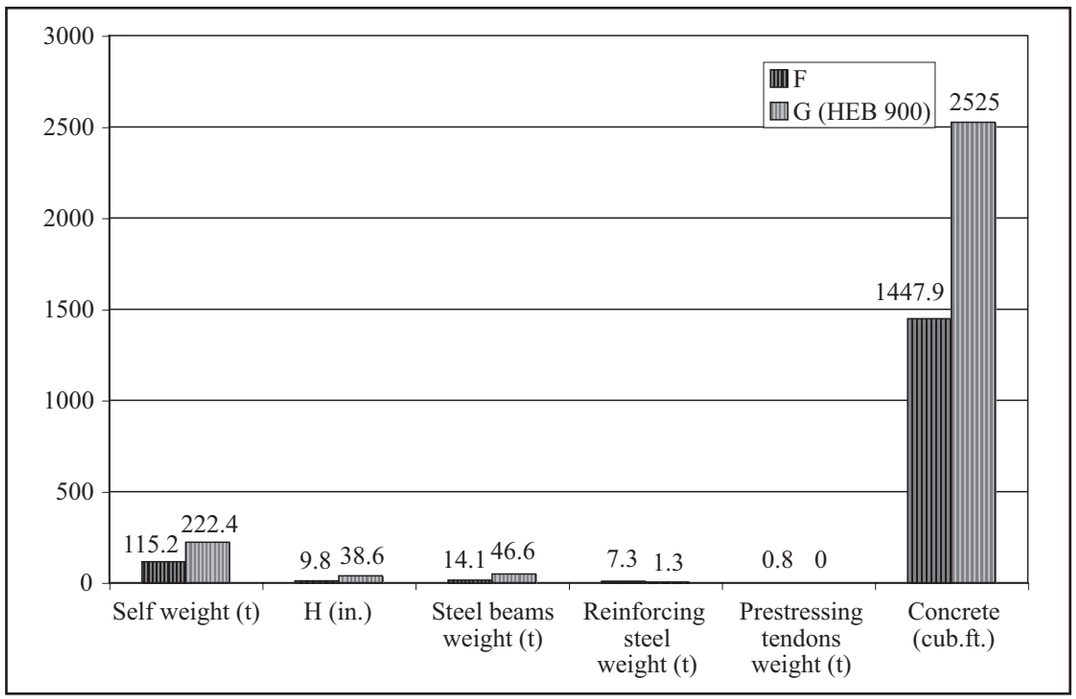

Fig. 20. Comparison between prestressed precambered U-shaped bridge deck, *F*, and encased girders, *G*.

Table 1. Summary of properties of the U-shaped bridge deck.

Span length	**59 to 85 ft (18 to 26 m)**
Total weight of a typical span of 85 ft (26 m)	164 tons (167 tonnes)
Price after production, waterproofing	
Typical span of 59 ft (20 m)	$75,000
Typical span of 85 ft (26 m)	$130,000
Weight of concrete	1.47 ton/ft (4.9 tonnes/m)
Weight of prestressing steel	0.0127 ton/ft (0.0425 tonnes/m)
Weight of steel girders	0.2144 ton/ft (0.715 tonnes/m)
Weight of mild steel reinforcement	0.11 ton/ft (0.37 tonnes/m)

- Aggregates (crushed limestone): 1922 lb per cu yd (1140 kg/m^3)
- Portland cement (CEMI52.5RLA, ASTM III, Class 3 CEB): 641 lb per cu yd (380 kg/m^3)
- Total water: 27.7 gallons per cu yd (137 L/m^3)
- Water reducing admixture (Visco 4): 11.8 lb per cu yd (7.0 kg/m^3)

Age of concrete at prestress transfer (release) – The histogram in Fig. 21 shows the age distribution (in hours) of the first phase concrete – when prebending of the steel girders took place and the prestressing force from the tendons was transferred.

Two peaks may be observed: the first peak occurs at 40 hours for the bridge decks heated at 113°F (45°C) during the first day after concreting of the bottom flange; the second peak occurs at 62 hours, corresponding mainly to non-heated [curing at an ambient temperature of about 68°F (20°C)] bridge decks. The minimal, mean, and maximal values of the age of concrete at prestress transfer are 30, 60 and 126 hours, respectively.

Compressive strength – The histogram in Fig. 22 shows the distribution of the average cube specimen compressive strength of the first phase concrete at prestress transfer. Fig. 23 represents the distribution of the average test specimen compressive strength of the concrete at 28 days. The minimal, mean, and maximal values of the compressive strength of concrete are 6672, 8093, and 10,805 psi (46, 55.8, and 74.5 MPa) at prestress transfer (release), and 9790, 11,356, and 12,763 psi (67.5, 78.3, and 88 MPa) at 28 days. The standard deviation of the compressive strength is 1015 psi (7 MPa) at prestress transfer and 725 psi (5 MPa) at 28 days.

Influence of curing temperatures – In order to more precisely understand the influence of heat curing on the compressive strength of the first phase concrete at prestress transfer and at 28 days, an analysis of variance was carried out. The analysis consisted of equality testing of the mean values for the test specimens with and without heat curing. The compressive strength at 28 days was found to be somewhat dependent on the heat curing (P-value = 0.055).

The P-value is the probability that there is no difference between the mean values. Usually, a difference between the mean values can be considered as significant when the P-value is less than 0.05. However, for the compressive strength at prestress transfer, no difference was found between the heated and non-heated first phase concretes (P-value = 0.828).

In the next statistical analysis, the data were divided into two groups: the first group for non-heat-cured concretes and the second group for heat-cured concretes. The box plot in Fig. 24 indicates the average compressive strength of the first phase concrete at prestress transfer for both curing

temperature groups. The mean values and the standard deviation for the concrete strength at prestress transfer are, respectively: 8151 and 928 psi (56.2 and 6.4 MPa) for the non-heated concretes, and 8079 and 1073 psi (55.7 and 7.4 MPa) for the heated concretes.

The box plot values in Fig. 25, however, reveal that the distribution of the average compressive strength for the first phase concrete at 28 days depends on curing temperatures [68°F (20°C) or 113°F (45°C)]. The minimal, mean, and maximal values of the average compressive strength of the first phase concrete at 28 days, without and with heat cure, are, respectively: 10,877, 11,676, and 12,763 psi (75, 80.5, and 88 MPa) and 9790, 11,168, and 12,618 psi (67.5, 77, and 87 MPa). The standard deviations without, and with heat cure, are 537 and 769 psi (3.7 and 5.3 MPa). The scatter of the results at 28 days is thus larger for concrete with heat cure than for concrete cured at ambient temperature.

First phase concrete stress versus strength – Another variable parameter linked to the concrete was suspected to have an influence on deck camber at prestress transfer: the ratio between the stress in the first phase concrete at the bottom fiber at midspan and the average compressive strength of the first phase concrete at prestress transfer. A statistical analysis was carried out on all the test data. The minimal, mean, and maximal values for this case were 23.5, 39.5 and 50.2 percent, and the standard deviation was 6.4 percent.

For some bridge decks, this stress-to-strength ratio can reach very high values, especially if one realizes that the concrete compressive strength is measured on cube specimens. Indeed, for this ratio, all data can be divided into two groups according to the type of steel girder used – welded or hot-rolled. The box plot in Fig. 26 shows that the mean value of this ratio is higher for bridge decks with welded steel girders (44.7 percent) than that for bridge decks produced with hot-rolled steel girders (37.5 percent).

Steel tensile stress versus strength – Three other continuous variables considered to be significant in deck camber were selected. The first variable is the ratio between the maximum tensile stress in the steel girders and the yield strength at prebending. The minimal, mean, and maximal values were 41.1, 67.1, and 74 percent. Again, the data were divided into two groups based on steel girder type.

The minimal, mean, and maximal values of this ratio for the group of welded steel girders and for the group of hot-rolled steel girders were 41.1, 50.6, and 69.5 percent, and 71.2, 72, and 74 percent, respectively. The standard deviations for the welded steel and hot-rolled steel girder groups were, respectively: 14 and 0.8 percent. This ratio is, therefore, strongly dependent

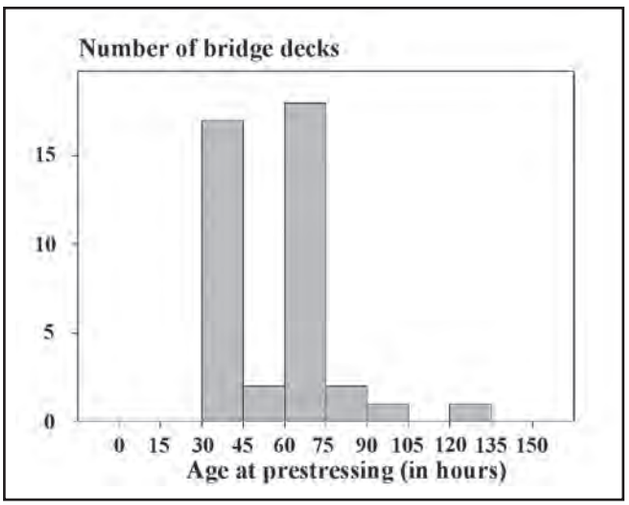

Fig. 21. Histogram of age distribution of first phase concrete at prestress release.

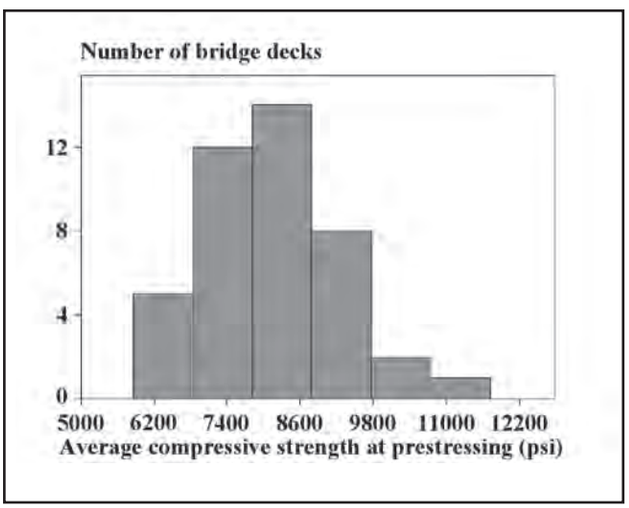

Fig. 22. Average cube compressive strength (psi) of first phase concrete at prestress release.

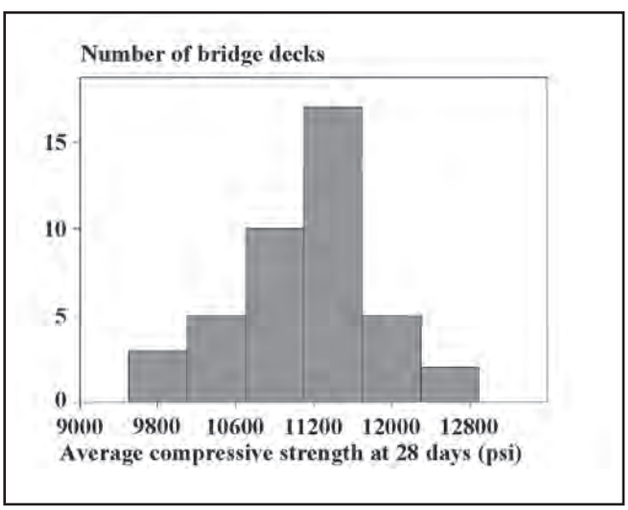

Fig. 23. Average cube compressive strength (psi) of first phase concrete at 28 days.

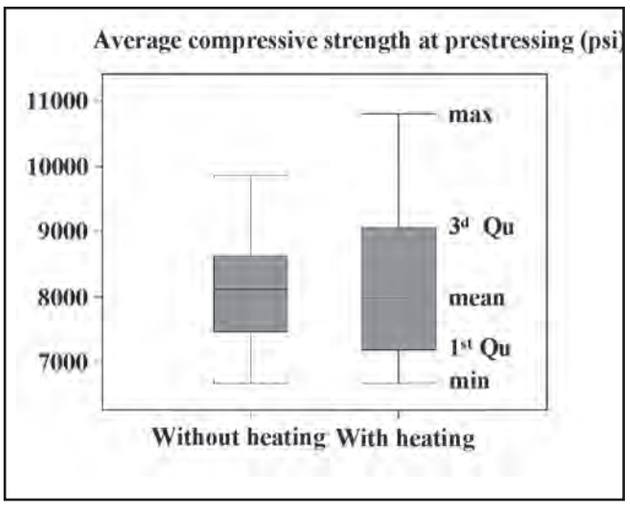

Fig. 24. Box plot of compressive strength of concrete (psi) at prestress release.

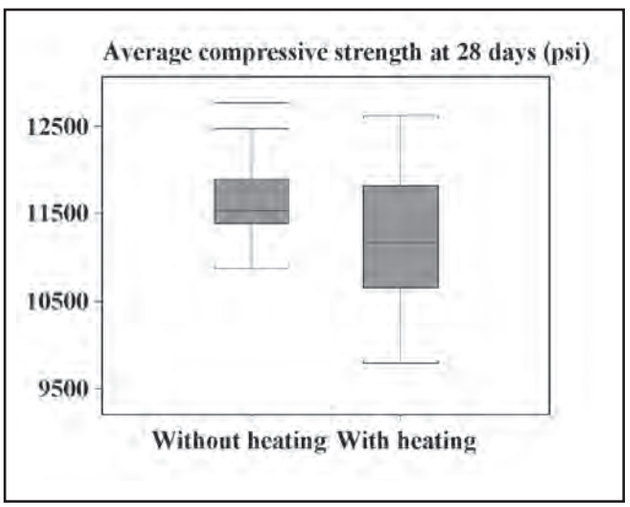

Fig. 25. Box plot of compressive strength of concrete (psi) at 28 days.

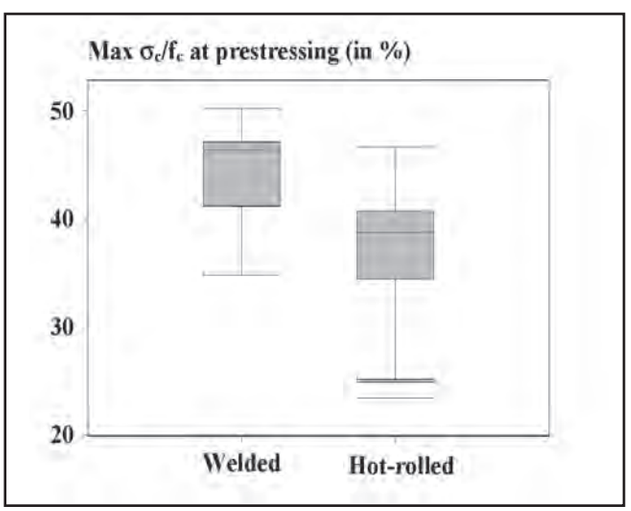

Fig. 26. Ratio between stress in concrete at bottom fiber at midspan and average cube compressive strength at prestress release (percent) for welded and hot-rolled steel girders.

on the type of steel girder used in deck production.

Steel compressive stress versus strength – The second continuous variable is the ratio between the maximum compressive stress in the steel girders and the yield strength at prebending. The minimal, mean, and maximal values were 32.9, 53.4 and 74 percent. When the data are divided into two groups according to steel girder type, the minimal, mean, and maximal values are 32.9, 40.2, 54.9, and 53.2, 57.2, 74 percent, respectively. This ratio is also strongly dependent on the manufacturing process of the steel girders.

Bending moment – The third continuous variable is the ratio between the external bending moment due to prestressing to the sum of the external bending moment due to prebending and the external bending moment due to prestressing. The minimal, mean, and maximal values of this ratio are 55.9, 71.7 and 79 percent; the standard deviation is 6.2 percent.

Statistical Analysis of Camber at Prestress Transfer

In order to explain the variability of the relative difference, *X*, between measured and computed camber just after prestress transfer, a statistical analysis of 42 bridge decks was performed using the following ten continuous or discrete variables:

1. Bottom slab concrete strength at age of prestress transfer, *A*
2. Curing temperature
3. Bottom slab concrete strength at 28 days, *B*
4. Age of concrete at prestress transfer, *C*
5. Type of steel girder used in production
6. Use of reinforcement in upper flanges of steel girders
7. Ratio of maximum tensile stress-to-yield strength in steel girders at prebending, *D*
8. Ratio of maximum compressive stress-to-yield strength in steel girders at prebending
9. Ratio of bending moment due to prestressing-to-the sum of bending moments due to prebending and prestressing, *E*
10. Ratio of maximum compressive stress in first phase concrete-to-first phase concrete strength at prestress transfer, *F*

An analysis of the principal components for the continuous Variables *A* through *F* identified the correlation matrix of pertinent variables for linear regression models (see Table 2).

The most significant variables are *D*, *B* and *C*, confirmed by the correlation between the continuous variables (see Fig. 27). Variable *X* is strongly correlated with Variable *D*.

The continuous Variables *B*, *C*, *D* and one discrete variable, namely, steel

girder type, were considered in a linear regression model in order to explain the variability of the camber at prestress transfer. The *P*-value is the probability that a given variable is not significant in explaining Variable *X*; typically, *P*-values less than 0.05 are considered statistically significant. Tables 3 and 4 show the results for two simulations.

Most significant variables – The maximum tensile stress-to-yield strength ratio in the steel girders at prebending, Variable *D*, and the steel girder type are the most significant variables in explaining the variability of the camber at prestress transfer. If the steel girder is hot-rolled and if the tensile stress-to-yield strength ratio in the steel girders at prebending is high, then the difference between the measured and computed cambers after prestress transfer is also high. For a maximum tensile stress higher than 70 percent of the yield strength, the yield strength can be reached with only the presence of residual stresses.

Furthermore, the hot-rolled steel girders are bent just after rolling, and contain more internal stresses than the welded steel girders. Therefore, the manufacturing process of the steel girders is significant due to its influence during the elastification phase, when residual stresses in the steel are removed. The box plot in Fig. 28 shows the variability of the camber at prestressing as a function of girder type. The mean values of the variability *X* for the bridge decks with hot-rolled and welded steel girders are 5.57 and 0.35 percent.

In Fig. 29, the variability of the camber, *X*, is plotted as a function of the maximum tensile stress-to-yield strength ratio in the steel girders at prebending, confirming the results of the previous statistical analysis. As a consequence of these results, the loss of camber by elastification should be taken into account accordingly in the design of these composite structures.

Fig. 30 also reinforces these conclusions, namely, that the measured permanent loss of steel girder camber after the elastification phase is higher for hot-rolled girders (mean value: 9.68 percent) than for welded steel girders (mean value: 5.21 percent).

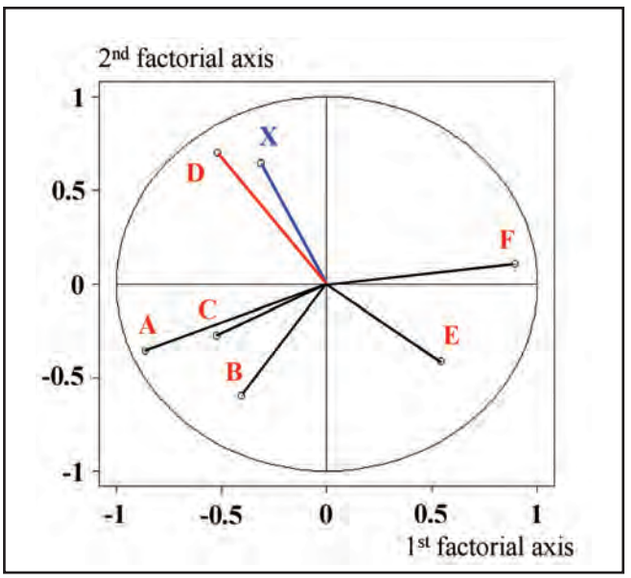

Fig. 27. Representation of continuous Variables *A* through *F* and *X*.

Table 2. Results of correlation matrix between Variables *A* through *F*, and *X*.

Variable	*A*	*B*	*C*	*D*	*E*	*F*
X	0.07	**- 0.255**	**0.218**	**0.47**	- 0.09	- 0.166

Table 3. Results of linear regression model with Variables *B, C, D* and *X*.

X	*B*	*C*	*D*
***P*-value**	0.058	0.077	**0.002**

Table 4. Results of linear regression model Variables *B, C, X,* and type of steel girder.

X	*B*	*C*	Steel girder type
***P*-value**	0.033	0.068	**0.005**

RESEARCH ON U-DECK TIME-DEPENDENT BEHAVIOR

Prestressing of the first phase concrete is transferred at an early age (2 or 3 days) and at high stress levels (about 0.5 $f'_{c,\,cube}$) on high strength concrete [$f'_{c,\,cube}$ = 6527 psi (45 MPa) at the age of prestress transfer]. The composite characteristic of the construction, with the combination between the high strength steel of the girders [A572 Grade (S355)], the steel of the prestressing tendons [Grade 270 (1860 MPa)], and the two phases of concreting should also be noted. These factors theoretically induce a significant time-dependent redistribution of internal stresses between steel and concrete, thereby reducing the prestressing of the bottom of the U-deck slab.

As noted earlier, the standard method for designing these bridge decks was a simple classical computation method with a modular ratio. However, this method produces an accurate solution of time-dependent effects only in the case of pure creep – and provides no stress redistribution analysis.

Since the above method furnishes only partial results, it was determined that an in-depth understanding of the influence of the concrete time-dependent effects in these types of composite structures was needed before proceeding with the design of the statically indeterminate bridge structure. The research presented in this paper was intended to provide experimental data to calibrate more advanced computational models.

Laboratory Investigation

A comprehensive experimental program was carried out in the civil engineering laboratory at the University of Brussels in order to better evaluate the concrete properties and provide data for an enhanced modelling of the time-dependent behavior of bridge decks. In

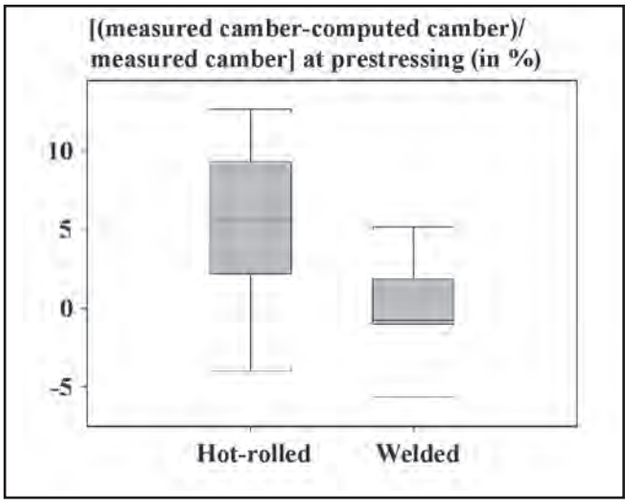

Fig. 28. Ratio between measured camber minus computed camber-to-measured camber at prestress release (in percent) for hot rolled and welded steel girders.

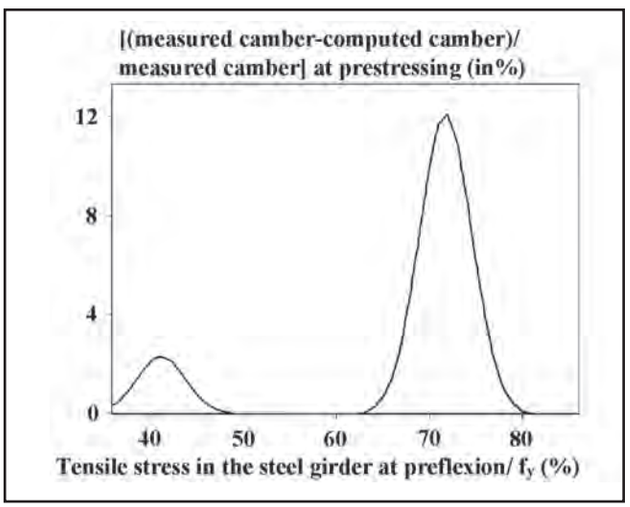

Fig. 29. Graph of the ratio between measured camber minus computed camber-to-measured camber at prestress release (in percent) as a function of tensile stress in steel girder-to-yield strength ratio (in percent).

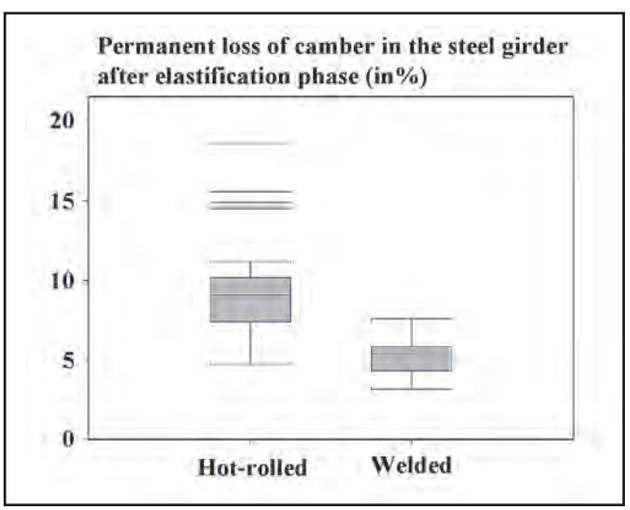

Fig. 30. Box plot of measured loss of camber in hot-rolled and welded steel girders after elastification.

particular, creep and shrinkage tests on cylinders – 6.0 in. (152 mm) diameter and 24 in. (610 mm) high test specimens – were performed following the recommendations issued by RILEM TC 107[6] under drying [68°F (20°C) and 53 percent relative humidity] and sealed conditions.

Creep and shrinkage testing – Creep specimens were loaded at various ages (2 days, 4 days, 7 days, 28 days, 6 months, and one year) and at different stress levels. Each creep specimen had a companion shrinkage specimen. This paper presents only the results from the autogenous shrinkage tests, the total shrinkage tests of specimens exposed to drying at 28 days, and the creep tests of specimens loaded at 28 days. The level of stress was 4076 psi (28.1MPa), corresponding to 44.4 percent of $f'_{c,\,28}$ = 9282 psi (64 MPa) for the first phase concrete, and 4114 psi (28.37 MPa), corresponding to 44 percent of $f'_{c,\,28}$ = 9353 psi (64.5 MPa) for the second phase concrete.

The creep and shrinkage curves recorded in the laboratory were compared with predictions obtained by several models.[10] For clarity in data representation, the authors focused on the CEB-MC 90 prediction model, either in its enhanced version (1999)[7] for high strength concrete, or in its originally published version (1993),[8] and on AFREM (issued by the French group of RILEM members) prediction model,[9] specifically developed for high strength concrete.

For sealed specimens, the relative humidity used in the CEB-MC90 (1993) Model Code was established at 98.99 percent. Above 99 percent relative humidity, this model assumes that swelling (expansion) occurs. The later CEB-MC90 (Version 1999) and the AFREM[9] models proposed an independent expression for the prediction of autogenous shrinkage. For creep in sealed specimens, the relative humidity used in the CEB-MC90 (1999) Model Code was set at 100 percent. The AFREM model utilized an independent expression for the fundamental creep prediction.

Fig. 31 graphs the predictions for autogenous shrinkage of the sealed and unloaded specimens. The experimental results generally follow the values predicted by the two models. However, the asymptotic value of the AFREM model appears a little low. Note also that the earlier CEB-MC90 (Version 1993) model does not adequately represent autogenous shrinkage in high performance concrete.[10]

The total shrinkage of the first and second phase concrete specimens exposed to drying at 28 days is plotted in Fig. 32. In this case, the scatter between the last measurements for both phase concretes is slightly lower than the differences between the predicted values. In actuality, the scatter of creep

and shrinkage test results for concretes from different batches may be quite large – even with a standard testing procedure and identical composition and constitutive materials.[11] The first phase concrete strains appear to follow the trend predicted by the 1999 version of the CEB-MC90 Model Code, whereas the second phase concrete strains are best represented by the 1993 version.

The prediction of the total creep function for unsealed specimens exposed to drying and loaded at 28 days is illustrated in Fig. 33. In this case, the experimental values fall between the values predicted by both versions (1999 and 1993) of the CEB-MC90 Model Code.

In the majority of creep and shrinkage tests (other exposure durations to drying or at loading), it is the CEB-MC90 Model Code, Versions 1993 and 1999, that best represent the shrinkage and creep deformations for this particular concrete; therefore, this model was used for numerical simulations. For autogenous shrinkage and fundamental creep, the 1999 version was found to best represent the time-dependent deformations of this concrete.

Site Investigation

In June 2000, a simply supported bridge deck with an 85 ft (26 m) span in a viaduct constructed at the entrance of the Brussels South Station was instrumented at one-third span and midspan locations. Resistive strain gauges were bonded to the steel girders and vibrating wire gauges were embedded in the concrete (see Figs. 34 and 35). For each instrumented section, two vibrating wire gauges were placed 3⅛ in. (80 mm) below the top section fiber, and four other gauges were set at 2.0 in. (51 mm) above the bottom section fiber.

Four resistive strain gauges were bonded to the bottom flanges of the girders and two others were installed on the upper flange of the girders. Strains have been recorded on these gauges since completion of the deck in June 2000. The reference point for strain measurements was established just prior to prebending of both steel girders.

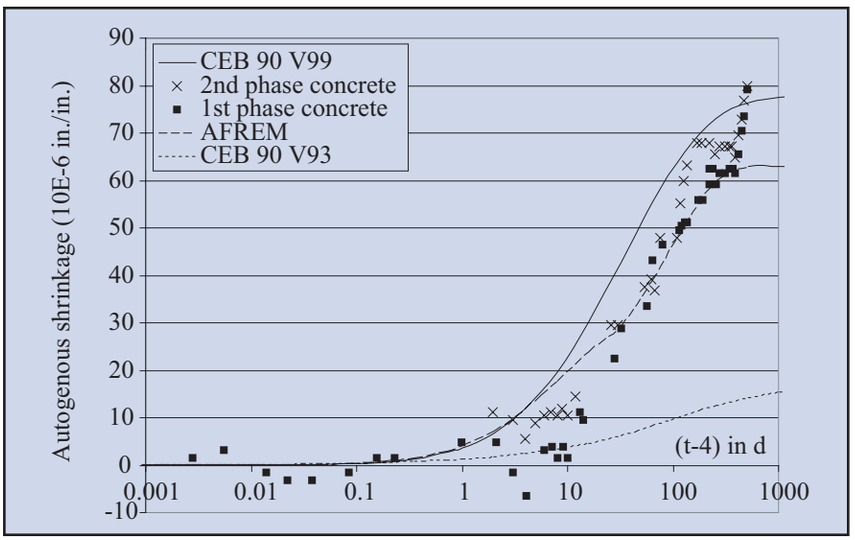

Fig. 31. Autogenous shrinkage strains (age of concrete at beginning of measurements: $t = 4$ days).

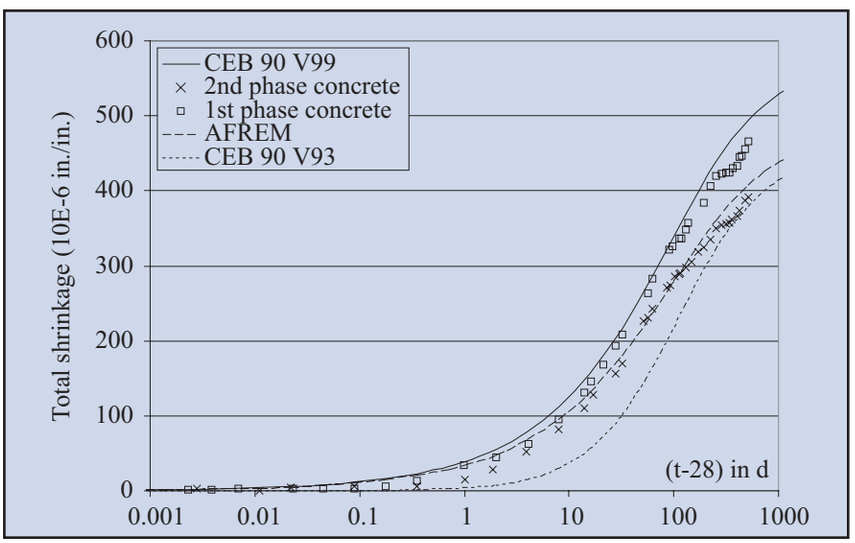

Fig. 32. Total shrinkage strains of specimens exposed to drying conditions at 28 days.

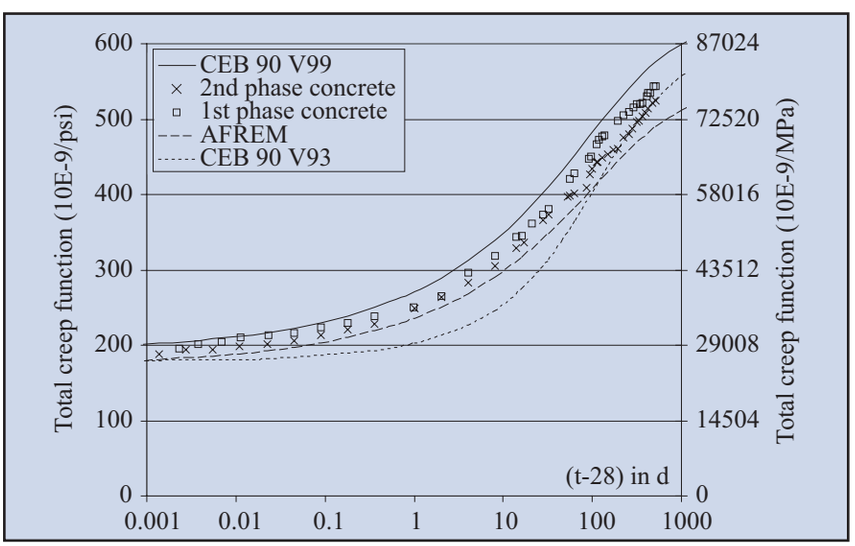

Fig. 33. Total creep function of specimens loaded at 28 days.

Comparison Between Measured and Computed Strains

This bridge deck, as those built previously, was designed with a simple classical computation method where the time-dependent effects are taken into account within the framework of a pseudo-elastic analysis with a variable modulus method. The modular ratios, *m*, were computed according to an empirical formula taken from the Belgian Standard NBN5 (1988) with *m* equal to: 5.59 after transfer of the prestressing force from the tendons (instantaneous value); 9.05 after transfer of the prestressing force from the tendons (long-term value); 9.05 for permanent loads (long-term value); and 4.97 for variable loads (instantaneous value).

Strains and stresses were computed in the following sequence:

(a) Immediately after prebending of the steel girders.
(b) Just after transfer of the prestressing force from the tendons.
(c) When the bridge deck was supported on temporary bearings.
(d) When the bridge deck was supported on its final bearings.
(e) After placement of the deck ballast.
(f) Under self-weight and the weight of ballast in the long-term.

These computed strains and stresses are indicated by the black squares in Figs. 36 to 40.

In this research, the age-adjusted effective modulus method (AEMM) and the step-by-step method[12] were used to evaluate the time-dependent behavior of the instrumented bridge deck. In the numerical simulation of this bridge deck, the shrinkage strains, modulus of elasticity, and creep coefficient were computed with the prediction model of the CEB-MC90 Model Code, Version 93.

The ageing coefficient in the age-adjusted effective modulus method was evaluated according to an expression proposed by Chiorino[13] in which the coefficient depends on the age at loading. The tension loss by relaxation in the tendons was evaluated according to the method proposed by Ghali and Trevino.[12, 14]

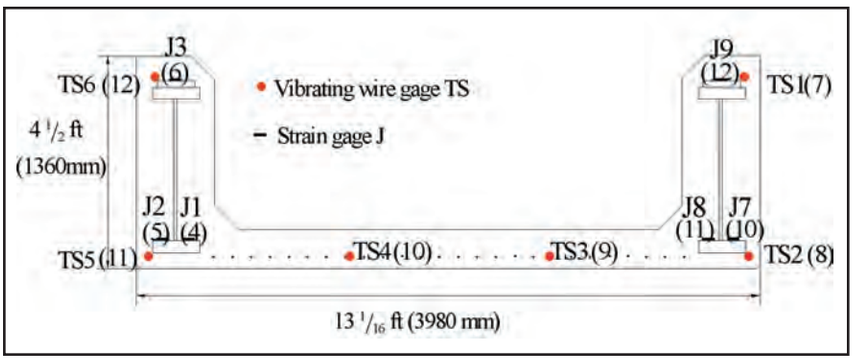

Fig. 34. Cross section of instrumented bridge deck with Gauges TS1 and J1 located at midspan and at one-third span.

Fig. 35. Bridge deck instrumented with strain gauges. (Photograph by Bernard Espion)

Fig. 36 shows the evolution of the strains in the steel at the level of the bottom flange, at one-third span. In Fig. 36, J*i* represents the measurement given by the *i*th strain gauge and TS*i* is the measurement given by the *i*th vibrating wire gauge. A positive strain value indicates extension, or expansion. The external relative humidity used in the computations was 80 percent.

Loading proceeded as follows:

1. Concreting of the bottom slab took place between 6 and 9 hours after prebending.
2. Prestressing occurred at $t = 2.5$ days.
3. Concreting of the webs (second phase concrete) took place at $t = 4$ days.
4. The deck was first stored in the prefabrication yard, and later transported by rail near the construction site.
5. The deck was placed on temporary supports (at one-fifth and four-fifths the span) between $t = 10$ and 45 days.
6. The deck was placed on its final bearings at $t = 45$ days.
7. The ballast was placed in two stages, at $t = 270$ days and at $t = 305$ days.
8. The viaduct was opened to service in June 2001.

In Fig. 36, very good agreement is apparent between the measured and computed strains in the steel at the level of the bottom flange, just after prebending of the steel girders; this result is not surprising since prebending occurs in an elastic state. A difference between the measured and computed

strains is noticeable just after the transfer of the prestressing force from the tendons. At this juncture, the concrete is 2½ days old and has already undergone considerable shrinkage.

The measurements show that the reinforcing steel was subjected to compression during this period due to concrete shrinkage. Note that shrinkage is not taken into account in the simple classical computation method (Belgian Standard NBN5), which was used in the earlier design of these bridge decks. However, the age-adjusted effective modulus method (AEMM) and the step-by-step method take shrinkage into account and produce good agreement with the results between measured and computed strains until placement on final bearings.

After the deck is placed on its final bearings, the step-by-step method appears to calculate much better the strain predictions than the AEMM. The step-by-step method evaluated more accurately the stress redistribution between the steel and the concrete over time than the AEMM. The values given by Strain Gauge J4 deviated significantly from the other data points.

Fig. 37 illustrates the strains in the first phase concrete in the slab at one-third span, showing observations similar to those noted before. After the placement of the deck on its final bearings (t > 45 days), the overestimate of the time-dependent effects with both methods was revealed. One possible explanation for this overestimate was the assumption of a constant relative humidity, when, in fact, the bridge deck undergoes a variable relative humidity with regard to waterproofing procedures.

After placement on its final bearings, some parts of the deck slab and webs were waterproofed. Therefore, the boundary conditions for concrete volume changes (desiccation) change over time. In parts of the concrete where the internal relative humidity is highest, creep and shrinkage strains are lower than strains near non-waterproofed surfaces.[15]

Fig. 38 illustrates the computed stresses for the first phase concrete in the slab. No tension appeared either with the age-adjusted effective modulus, the step-by-step method, or with the simple classical computation meth-

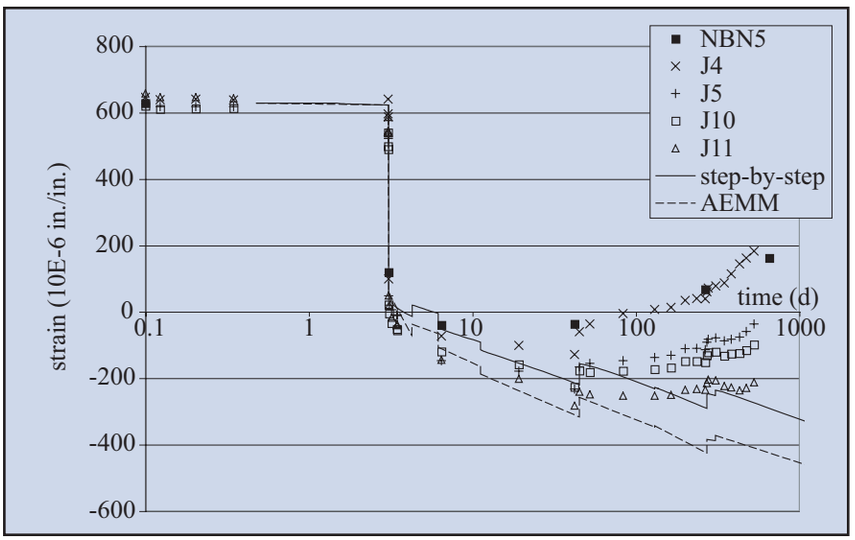

Fig. 36. Steel strains in girders at bottom flange level at one-third span.

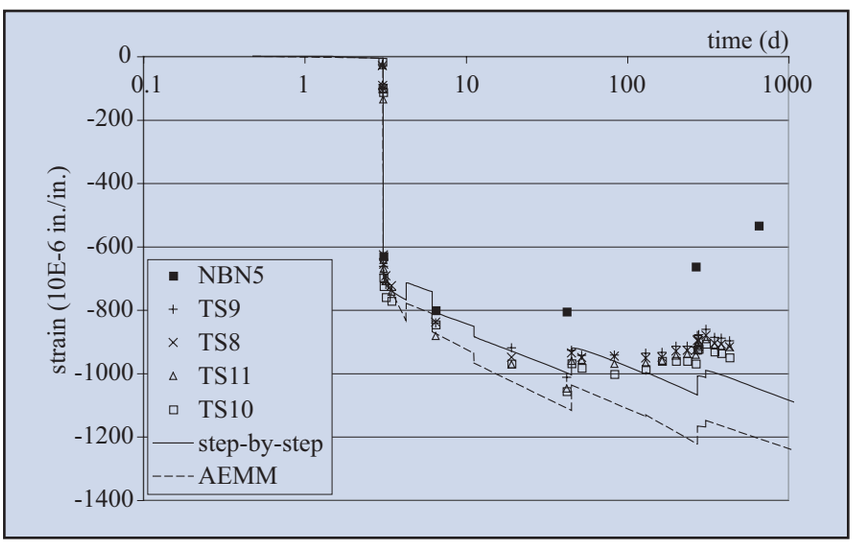

Fig. 37. Concrete strains in slab at 2 in. (50 mm) from bottom fiber at one-third span.

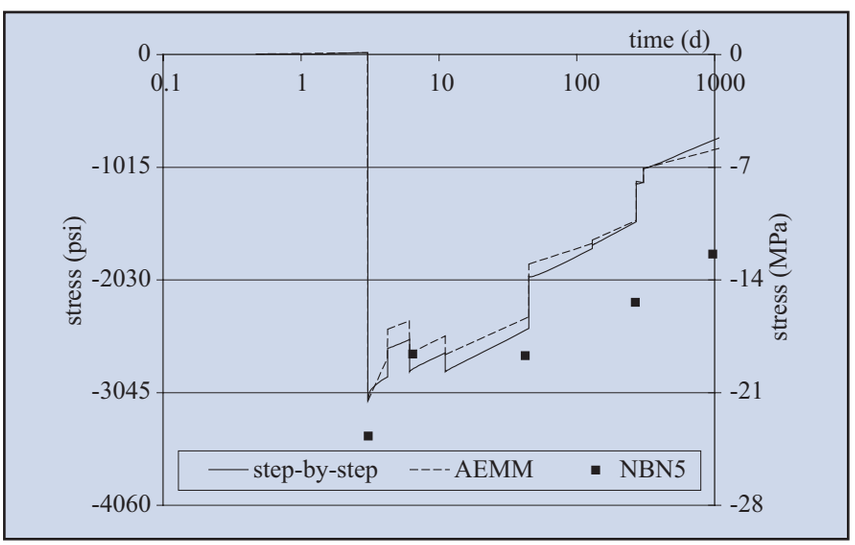

Fig. 38. Stresses in slab at 2 in. (50 mm) from bottom fiber at one-third span.

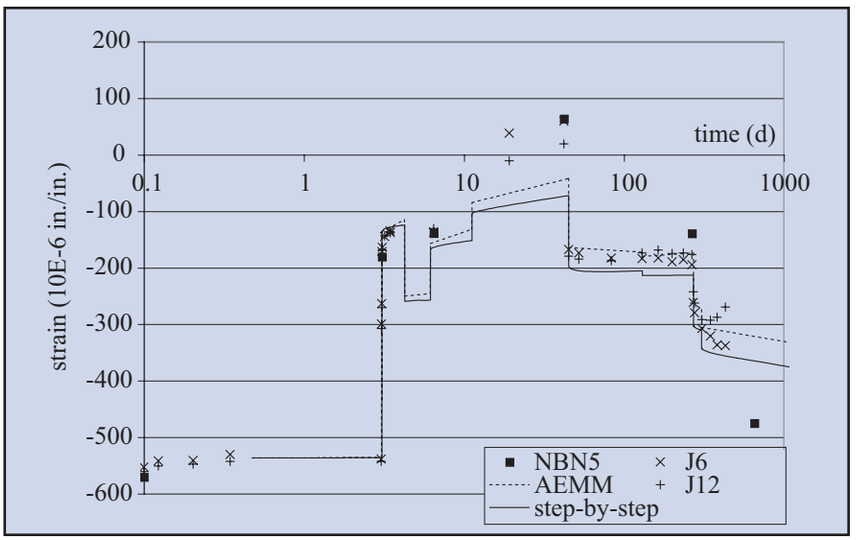

Fig. 39. Steel strains in girders at level of upper flange at one-third span.

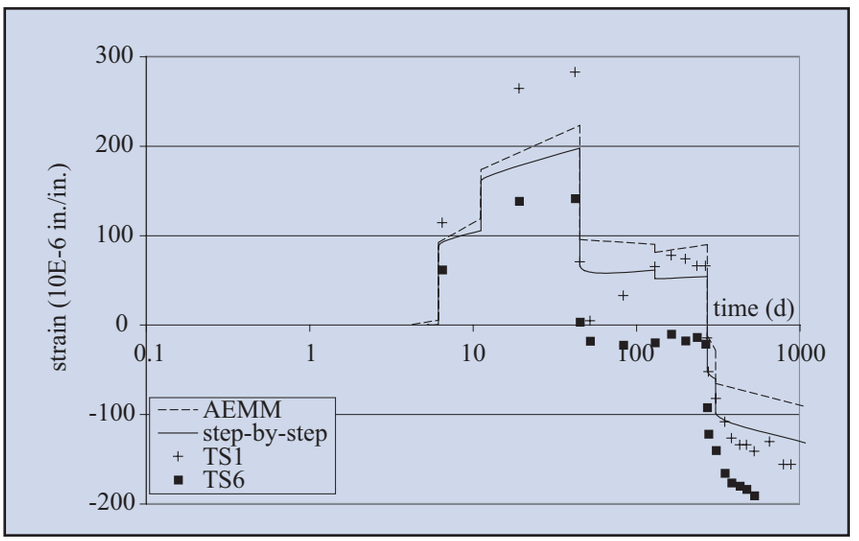

Fig. 40. Concrete strains in second phase concrete at ⅜ in. (80 mm) from upper fiber at midspan.

od (Belgian Standard NBN5) used in earlier designs of these bridge decks. The simple classical computation method, however, underestimated significantly the prestressing losses in the slab.

Note in Fig. 39 that good agreement was found between measured and computed strains in the girders (at the upper flange at one-third span) by the age-adjusted effective modulus and step-by-step methods. The same agreement is evidenced in Fig. 40, in particular, the result produced by the step-by-step method in the second phase concrete [at 3⅛ in. (80 mm) below the upper fiber at midspan].

CONCLUDING REMARKS

When the expansion and upgrading works for the Brussels South Station high speed rail lines commenced in the early 1990s, more than 2 miles (3 km) of viaducts with single track had to be built in a congested urban environment. For the success of this complex project, several specifications had to be met; of particular importance was the need to design bridge decks with a minimal construction depth, while ensuring minimal disturbance to the surrounding infrastructure and urban transportation during construction. An innovative solution met these project mandates, namely, by the use of a prefabricated, prestressed precambered composite U-shaped bridge deck.

By comparing the U-shaped bridge deck to other sections without precambered steel girders, this project has demonstrated that longer spans [up to 92 ft (28 m)] may be realized by using precambered steel girders and prestressing, simultaneously. Nearly 400 U-shaped bridge decks have been built in Belgium in recent years and all these structures have performed according to expectations. However, some variability has been observed between the measured camber at prestress transfer and camber as computed by the classical computation method using a pseudo-elastic analysis with imposed modular ratios.

Neither the compressive strength of the first phase concrete at prestress transfer – nor the compressive strength of the first phase concrete at 28 days – was found to have a statistically significant influence on the variability of the camber. Indeed, the most significant variables to explain camber measurement discrepancies at prestress transfer are the maximum tensile

stress-to-yield strength ratio in the steel girders at prebending, and the steel girder type.

In addition, the measured permanent loss of camber in the steel girders after the elastification phase was shown to be higher for hot-rolled girders than for welded steel girders. To increase the accuracy of the camber computation at prestress transfer, the design method should take into account the steel girder manufacturing process to properly evaluate the loss of camber after the elastification phase.

In an instrumented bridge deck, the authors found that the computed strain values derived from an approximate, pseudo-elastic analysis with imposed modular ratios are quite different from the measured strains – especially 2½ years after construction. The values computed by the step-by-step method show a better agreement with the measured strains than the values computed by the age-adjusted effective modulus method.

In general, the step-by-step method is a more precise evaluator of the time-dependent redistribution of strains between steel and concrete than the age-adjusted effective modulus method. However, these methods have some limitations. In addition to the basic assumptions of both methods – regarding the numerical evaluation of the classical integral of the principle of superposition and the applicability of this principle – the authors would like to emphasize the following point: the average section behavior hypothesis in relation to concrete volume change assumes that the relative humidity remains constant, when, in fact, the bridge deck experiences variable humidity conditions especially with regard to waterproofing procedures.

The results of this research have been successful in developing a more accurate estimate of time-dependent effects in concrete for composite, complex structures with a variable loading history. The continuation of this research will focus on the development of a numerical simulation that takes into account the local evolution of concrete bridge deck volume change due to the process of desiccation over time.

ACKNOWLEDGMENTS

A portion of this research was financed by a grant funded by the Belgian National Foundation for Scientific Research, and this is gratefully acknowledged. The authors also wish to thank our colleagues, O. Germain and C. Jadoul, and the organizations of RONVEAUX s.a. and TUCRAIL s.a. for their close collaboration throughout this project. Finally, the authors want to express their appreciation to the editors of the PCI JOURNAL for their helpful comments in improving the clarity of the paper.

REFERENCES

1. Baes, L., and Lipski, A., "La poutre Préflex, la décompression du béton enrobant l'aile tendue, le problème du retrait et du fluage," *Revue C* (Gent), No. 1-4, 1957, pp. 29-49.
2. Novgorodsky, L., "La Tour du Midi à Bruxelles, immeuble pour bureaux de 37 étages et de 150 mètres de hauteur," *La Technique des Travaux* (Liège), No. 11-12, 1966, pp. 322-335.
3. Verkeyn, A., and Dobruszkes, A., "Le centre administratif Berlaymont," *Annales des Travaux Publics de Belgique* (Brussels), No. 1-2, 1978, pp. 136-139.
4. Dekeyser, R., Ledent, H., Daoust, A., and Counasse, C., "La poutre mixte préfléchie et précontrainte (Flexstress) dans le cadre du pont sur le barrage de Lixhe," *Annales des Travaux Publics de Belgique* (Brussels), No. 3, 1990, pp. 165-198.
5. Couchard, I., and Detandt, H., "Entrance of the High Speed Line in the Brussels South Station," *Proceedings*, 16th IABSE Congress, Lucerne, Switzerland, 2000.
6. RILEM TC 107-CSP, "Measurement of Time-Dependent Strains of Concrete," *Materials and Structures (RILEM)*, V. 31, 1998, pp. 507-512.
7. Müller, H. S., Küttner, C. H., and Kvitsel, V., "Creep and Shrinkage Models of Normal and High Performance Concrete – Concept for a Unified Code-Type Approach," *Revue française de génie civil* (Paris), V. 3, No. 3-4, 1999, pp. 113-132.
8 *CEB-FIP Model Code 1990*, Bulletin CEB, No. 213/214, Thomas Telford, London, 1993.
9. Le Roy, R., de Larrard, F., and Pons, G., "Calcul des déformations différées des bétons à hautes performances," *Bulletin des Laboratoires des Ponts et Chaussées* (Paris), Spécial XIX, 1996, pp. 63-84.
10. Staquet, S., Detandt, H., and Espion, B., "Time-Dependent Behaviour of a Railway Prestressed Composite Bridge Deck," *Proceedings*, International Conference Concreep-6@MIT, F.-J. Ulm, Z. P. Bažant and F. H. Wittmann, Editors, Elsevier, Paris, 2001, pp. 373-378.
11. Staquet, S., and Espion, B., "On Variability of Measured Strains in Creep and Shrinkage Tests," *Proceedings*, International Conference Concreep-6@MIT, F.-J. Ulm, Z. P. Bažant and F. H. Wittmann, Editors, Elsevier, Paris, 2001, pp. 729-734.
12. Ghali, A., Favre, R., and Elbadry, M., *Concrete Structures: Stresses and Deformations*, Third Edition, E&FN Spon, Amsterdam, 2002.
13. Chiorino, M. A., *CEB Design Manual*, "Structural Effects of Time-Dependent Behaviour of Concrete," *Bulletin d'information du CEB*, No. 215, 1993, pp. 269-271.
14. Ghali, A., and Trevino, J., "Relaxation of Steel in Prestressed Concrete," PCI JOURNAL, V. 30, No. 5, 1985, pp. 82-94.
15. Staquet, S., "Analyse et modélisation du comportement différé du béton. Application aux poutres mixtes, préfléchies et précontraintes ," Ph.D. Thesis, University of Brussels, Brussels, Belgium, 2004.